Biogeochemistry **66:** 171–186, 2003.

On the possibility for generic modeling of submarine groundwater discharge

GEORGIA DESTOUNI[1,*] and CARMEN PRIETO[2]

*[1]Department of Physical Geography and Quaternary Geology, Stockholm University, SE-106 91 Stockholm, Sweden; [2]Department of Land and Water Resources Engineering, KTH, Brinellv 32, S-100 44 Stockholm, Sweden; *Author for correspondence*

Key words: Coastal aquifer, Coastal zone, Groundwater–seawater interactions, Seawater intrusion, Submarine groundwater discharge

Abstract. We simulate large-scale dynamics of submarine groundwater discharge (SGD) in three different coastal aquifers on the Mediterranean Sea. We subject these aquifers to a wide range of different groundwater management conditions, leading to widely different net groundwater drainage from land to sea. The resulting SGD at steady-state is quantifiable and predictable by simple linearity in the net land-determined groundwater drainage, defined as total fresh water drainage minus groundwater extraction in the coastal aquifer system. This linearity appears to be general and independent of site-specific, variable and complex details of hydrogeology, aquifer hydraulics, streamlines and salinity transition zones in different coastal systems. Also independently of site-specifics, low SGD implies high seawater content due to seawater intruding into the aquifer and mixing with fresh groundwater within a wide salinity transition zone in the aquifer. Increasing SGD implies decreasing seawater content, decreased mixing between seawater and fresh groundwater and narrowing of the salinity transition zone of brackish groundwater in the aquifer.

Introduction

In coastal aquifers, intruding seawater through the free connection to the sea may be mixed with and measurably diluted by fresh groundwater derived from land drainage. Such a dynamic mixing zone constitutes also a zone of salinity transition, from fresh groundwater to pure seawater and has been described as a subterranean estuary that may be of great importance for coastal ecosystems by supplying brackish groundwater, along with chemical tracers and nutrients to the coastal waters (Buddemeier 1996; Moore 1996, 1999). The definition of submarine groundwater discharge (SGD) from this salinity transition zone into the sea, however, has been ambiguous and led to yet unresolved discussions in the literature about the actual magnitude of SGD and its appropriate quantification (Moore 1996; Moore and Church 1996; Younger 1996; Li et al. 1999; Uchiyama et al. 2000).

Moore (1996) argued that SGD must have been the main source of observed enriched ^{226}Ra concentrations in coastal waters of the South Atlantic Bight, yielding an SGD estimate for the investigated coastline and time period of about 40% of the river water flow into the same coast. In absolute terms, this SGD estimate was about $3{\cdot}10^7\,m^3\,day^{-1}$, distributed over a coastline length of about

320 km. Younger (1996) argued from a hydrological and groundwater hydraulic basis that there is neither sufficient groundwater recharge, nor the required combination of hydraulic conductivity and hydraulic gradient in the considered coastal aquifer to even come close to supporting such a high SGD estimate. Younger (1996) also argued that density driven groundwater dynamics in the transition zone between fresh and salt water cannot support a fresh water seepage zone that has greater seaward extent than a couple of 100 m at the maximum. This extent should then be compared to the landward seepage zone of 20 km, required for making the estimated total SGD rate of $3 \cdot 10^7\,m^3\,day^{-1}$ consistent with measured submarine groundwater fluxes at the coast of North and South Carolina, which are in the range of $5–20\,l\,m^{-2}\,day^{-1}$ (Simmons 1992). Moore and Church (1996) replied that there is great uncertainty in both groundwater recharge and groundwater flux estimates, and that total SGD does not only include fresh groundwater discharge, but also seawater that intrudes into the aquifer and then flows back into the sea mixed with the fresh groundwater.

Li et al. (1999) suggested that temporal variability in the seawater component of SGD, due to sea-level fluctuations by tide and wave setup may explain the observed excess ^{226}Ra transport into the coastal waters of the South Atlantic Bight even for low average SGD. Uchiyama et al. (2000), however, simulated in detail SGD under realistic conditions of tidal fluctuations, finding both SGD and the associated desorbed nutrient transport to be minor in comparison to the river flow and transport in the investigated area.

In general, SGD investigations have thus so far opened and left open a series of questions regarding the quantification of total SGD, its possible division into a freshwater and a seawater component, the temporal variability of these two components and the tracer transport that the SGD may carry with it to the coastal water. The objective of the present paper is to shed light on and answer some of these open questions about the SGD quantification, by using, comparing and combining SGD results from different site-specific numerical simulations of fresh water outflow and associated seawater intrusion and outflow back into the sea in coastal aquifers.

Materials and methods

General methodology

We have simulated the groundwater dynamics and resulting SGD in three different coastal aquifers on the Mediterranean Sea, which also constitute well-investigated case studies of the EU research project WASSER (Utilisation of Groundwater Desalination and Wastewater Reuse in the Water Supply of Seasonally-Stressed Regions; see Koussis 2001; Prieto 2001; Prieto et al. 2001; Koussis et al. 2002). These aquifers are the Coastal aquifer in Israel, the Tsairi basin aquifer on the island of Rhodes in Greece and the Akrotiri aquifer in Cyprus. Within the WASSER project, a representative aquifer-sediment cross-section was conceptualized and quantified for conditions considered typical for each coastal region and we in-

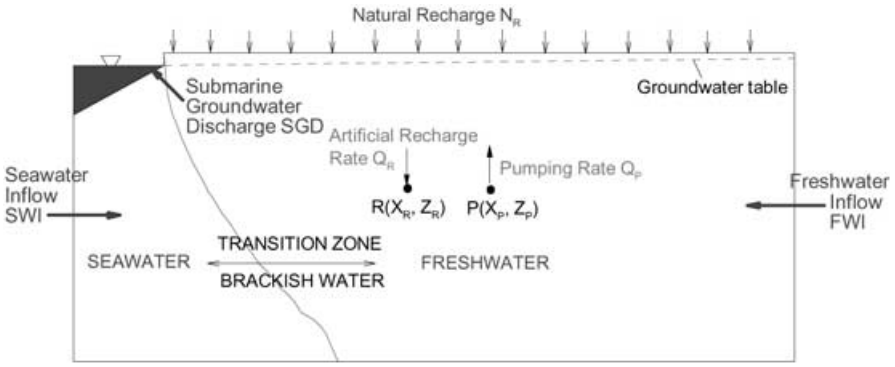

Figure 1. Schematic representation of main common features common to all modeled aquifer-sediment cross-sections, including illustrative definitions of coastline integrated and averaged boundary and managed system flow rates and representative pumping, $P(X_P,Z_P)$, and artificial recharge, $R(X_R,Z_R)$, well positions.

vestigated the resulting groundwater dynamics in these cross-sections for different groundwater management scenarios (in terms of pumping and artificial infiltration) by use of the coupled water flow and transport simulation model SUTRA (Voss 1984).

Figure 1 illustrates schematically some main common features for all three site-specific simulation cross-sections, along with the overall boundary and managed groundwater flow rates that generally drive the resulting SGD, defined as the total mixture of seawater and fresh groundwater flowing out from the aquifer, into the coastal water, through the underlying sediments. These boundary and managed flow rates are: FWI, the freshwater inflow rate through the landside boundary (specified directly, or determined by a specified water pressure in the different simulations); N_R, the effective (infiltration from rainfall, minus evapotranspiration and surface runoff) natural recharge rate through the soil surface boundary; SWI, the seawater inflow at the seaside boundary (due to the specified seawater level there, in conjunction with the hydraulic conditions within the simulated cross-section); Q_P, the pumping, or extraction rate of groundwater; and Q_R, the potential artificial groundwater recharge of treated waste water. When steady-state conditions are established in the different simulations, all these different input and output flow rates must be in dynamic equilibrium over the total simulated flow domain and the water balance relation between them is:

$$\mathrm{FWI} + N_R + Q_R + \mathrm{SWI} = Q_P + \mathrm{SGD} \tag{1}$$

with the left hand side summarizing all the input flows and the right hand side all the output flows for the simulated aquifer-sediment cross-section.

In terms of salt concentration, the landside input flows FWI, N_R and Q_R contain only freshwater (TDS concentration ≤ 500 ppm), and the seaside input flow SWI only seawater (TDS concentration of 35,000 ppm). The land and seaside output

flows, Q_P and SGD, respectively, however, might at steady-state be any resulting mixture of salt and fresh groundwater, depending on the simulated groundwater management practices and boundary conditions. In addition to the water balance expressed by Equation (1), we may express the balance of salt transport at steady-state as:

$$(\mathrm{SGD_F} + \mathrm{SGD_{SW}}) \cdot c_{\mathrm{SGD}} = \mathrm{SGD_F} \cdot c_{\mathrm{F}} + \mathrm{SGD_{SW}} \cdot c_{\mathrm{SW}} \tag{2}$$

where $\mathrm{SGD_F}$ and $\mathrm{SGD_{SW}}$ are the components of fresh groundwater and seawater in the total SGD, respectively, such that $\mathrm{SGD} = \mathrm{SGD_F} + \mathrm{SGD_{SW}}$, and c_{SGD}, c_{F} and c_{SW} are the salt concentrations in total SGD, the fresh groundwater component and the seawater component, respectively. By re-arranging (2), we then arrive at the following expression of the fresh groundwater and sea water component fractions of SGD, $\mathrm{SGD_F/SGD}$ and $\mathrm{SGD_{SW}/SGD}$, respectively:

$$\frac{\mathrm{SGD_F}}{\mathrm{SGD}} = \frac{1}{1 + (c_{\mathrm{F}} - c_{\mathrm{SGD}})/(c_{\mathrm{SGD}} - c_{\mathrm{SW}})}, \qquad \frac{\mathrm{SGD_{SW}}}{\mathrm{SGD}} = 1 - \frac{\mathrm{SGD_F}}{\mathrm{SGD}} \tag{3}$$

which can thus be evaluated from known fresh water, c_F, and seawater, c_{SW}, concentrations and the resulting SGD salt concentration, c_{SGD}, in different case study and groundwater management simulation scenarios.

The physical interpretation of the different flow rates in Equation (1), within the considered two-dimensional simulation domain (Figure 1), is that they all represent large-scale coastal system variables, which are appropriately integrated over coastline length, seepage zone extent and time, in order to represent annual and coastline averaged quantities. They vary between different case study and management scenario combinations, but are, at steady-state, constant for each such combination (i.e., they will be representative constants for each coastal groundwater management scenario at steady-state). In the following subsection, we describe how such large-scale input values can be independently estimated for a site-specific case study.

Site-specific simulations

Figure 2 illustrates the three different site-specific aquifer-sediment cross-sections, along with some key input data, initial and boundary conditions for each investigated site. Table 1 lists all the physical and numerical parameter values used in the SUTRA simulations, which along with the input specifications shown in Figure 2 remain the same for all considered water management scenarios for each site.

For the site-specific N_R and FWI inputs, we have used the catchment-representative hydrologic and groundwater management quantifications made and used within the WASSER project, with detailed quantification descriptions being reported by Koussis (2001), Prieto (2001), Prieto et al. (2001), Koussis et al. (2002). In summary, N_R was in the Israel case (Figure 2(a), Table 1) estimated based on local data records of rainfall and evapotranspiration (Tahal 1999), with the boundary inflow rate FWI being, in this case, a simulation output variable, depending on the specified boundary water pressure (based on site-specific hydro-

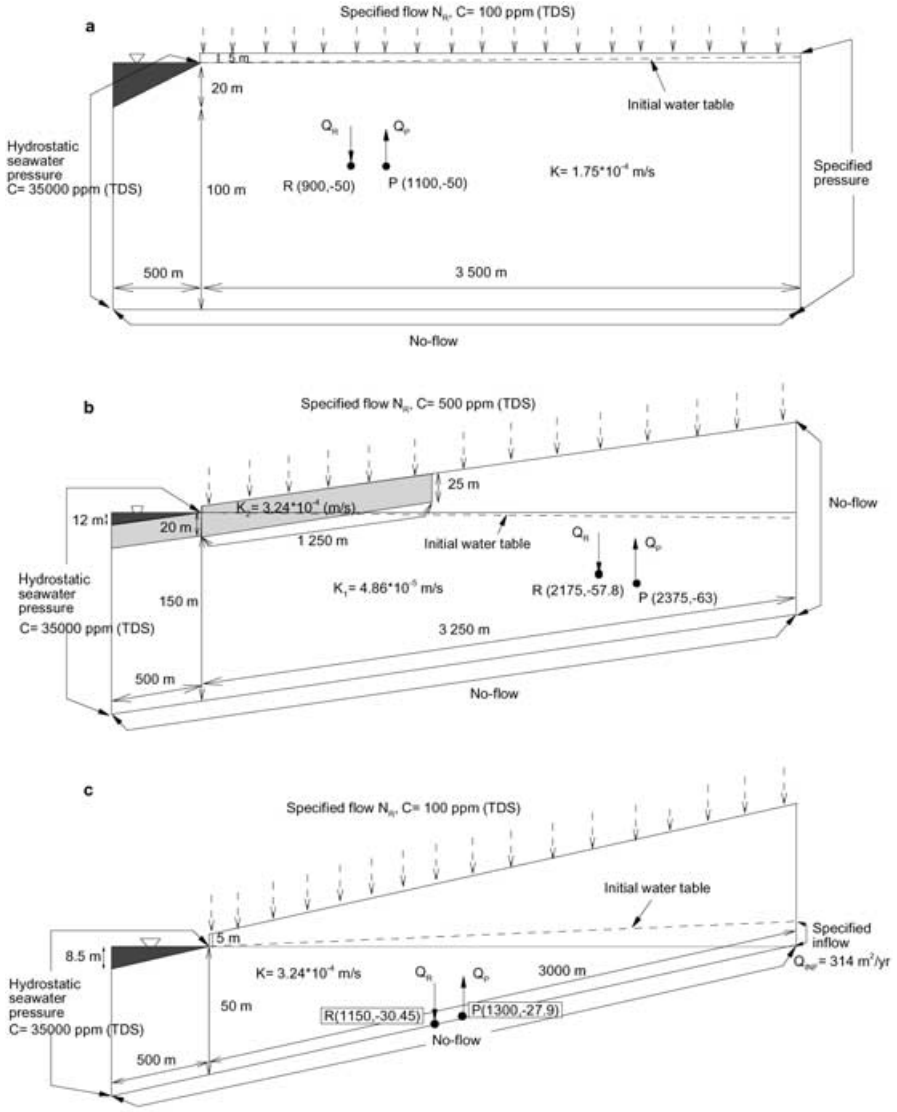

Figure 2. Site-specific simulated aquifer-sediment cross-section for: (a) the Israel case study, (b) the Rhodes case study, and (c) the Cyprus case study; the pumping and artificial recharge well positions, $P(X_P, Z_P)$ and $R(X_R, Z_R)$, respectively, are given in meters, quantifying horizontal distance from shoreline for the X coordinate and vertical distance from sea level for the Z coordinate; the Q_P, Q_R and N_R definitions are as in Figure 1.

geological data records) and resulting hydraulic conditions within the simulation domain. In the Rhodes case (Figure 2(b), Table 1), N_R was estimated from applying and calibrating the hydrologic model SWAT (Soil and Water Assessment Tool, Neitsch et al. 1999) on available hydrologic data for the Tsairi basin; the boundary

Table 1. Physical and numerical parameter values used in the SUTRA simulations for the three case studies.

Parameter	Israel	Rhodes	Cyprus
Length of simulated cross-section (m)	4000[a]	3750[a]	3500[a]
Representative width of simulated cross-section (m)	16000	2500	4000
Formation (unsaturated and saturated zone) depth[b] (m)	125	175	55
Mean unsaturated zone depth[c] (m)	≈ 3	≈ 20	≈ 25
Number of elements	2200	3710	1640
Number of nodes	2375	3886	1793
Spatial discretisation			
Horizontal, Δx (m)	25	25	25
Vertical 1: Δy_1 (m)	2.5[d]	2.5[e]	2.5[f]
Vertical 2: Δy_2 (m)	10[g]	10[h]	5[i]
Mean effective natural groundwater recharge N_R (m^3 $year^{-1}$ m^{-1})	707	282	249
Mean saturated hydraulic conductivity (m/s)	$1.75 \cdot 10^{-4}$	$4.86 \cdot 10^{-5}$[j]	$3.24 \cdot 10^{-4}$
Effective porosity	0.36	0.36	0.2
Longitudinal dispersivity (m)	12.5	12.5	12.5
Transverse dispersivity (m)	1.25	1.25	1.25
Fluid compressibility	0	0	0
Fluid viscosity (kg m^{-1} s^{-1})	10^{-3}	10^{-3}	10^{-3}
Aquifer matrix compressibility	0	0	0
Parameter a in Van Genuchten equation ($m\,s^2\,kg^{-1}$)	$5 \cdot 10^{-5}$	$5 \cdot 10^{-5}$	$5 \cdot 10^{-5}$
Parameter n in Van Genuchten equation	2	2	2
Residual degree of saturation	0.3	0.3	0.3
Molecular diffusivity of solute in fluid ($m^2\,s^{-1}$)	10^{-9}	10^{-9}	10^{-9}
Base solute concentration (ppm TDS)	100	500	100
Freshwater density ($kg\,m^{-3}$)	998.275	998.575	998.275
Seawater density ($kg\,m^{-3}$)	1024.45	1024.45	1024.45
Density change with concentration coefficient ($kg^2\,kgTDS^{-1}\,m^{-3}$)	750	750	750

[a]Of which 500 m is on the seaside; over this length, the sea depth goes from 0 to 20 m in Israel, from 0 to 12 m in Rhodes, and from 0 to 8.5 m in Cyprus.
[b]On the landside.
[c]Varies in time and space.
[d]For elements above sea level.
[e]For elements within the uppermost soil layer of 25 m.
[f]For elements within the uppermost soil layer of 5 m.
[g]For elements below sea level.
[h]For elements below the uppermost soil layer of 25 m.
[i]For elements below the uppermost soil layer of 5 m.
[j]The uppermost soil layer of 25 m in the Rhodes case has differing hydraulic conductivity of $3.24 \cdot 10^{-4}\,m\,s^{-1}$

inflow rate FWI was in this case specified to be zero, based on the assumption that future upstream groundwater management practices would not allow for any substantial groundwater inflow into the simulated coastal groundwater system. In the Cyprus case (Figure 2(c), Table 1), both N_R and the specified boundary inflow value FWI were obtained from the hydrological PRMS model (Precipitation–Runoff Modeling System; Leavesley et al. 1983; Leavesley and Stannard 1995), operated

Table 2. Simulated groundwater management scenarios for the three case studies.

Israel			Rhodes			Cyprus		
Q_P ($m^2\,year^{-1}$)	Q_R ($m^2\,year^{-1}$)	Resulting Q_N ($m^3\,year^{-1}\,m^{-1}$)	Q_P ($m^2\,year^{-1}$)	Q_R ($m^2\,year^{-1}$)	Resulting Q_N ($m^3\,year^{-1}\,m^{-1}$)	Q_P ($m^2\,year^{-1}$)	Q_R ($m^2\,year^{-1}$)	Resulting Q_N ($m^3\,year^{-1}\,m^{-1}$)
946	0	91	1010	0	−728	1000	0	−437
946	120	180	1010	364	−364	1000	218	−218
946	239	269	505	0	−223	1000	437	0
946	359	358	1010	728	0	375	0	188
946	478	448	1010	1092	364	1000	656	218
0	0	742	1010	1456	728	1000	874	437
946	1500	1208	1010	2028	1300	1000	1937	1500
946	2300	1802	1010	3128	2400	1000	2437	2000
946	3400	2628	1010	4728	4000	1000	4437	4000
946	6000	4560	1010	5728	5000	1000	5437	5000
946	8000	6044	1010	7228	6500	1000	6437	6000
946	10000	7524				1000	7437	7000
						1000	10437	10000

within the USGS'MMS (Modular Modeling System; Leavesley et al. 1996a,b; Leavesley et al. 2002) and calibrated for the considered catchment.

Using the thus specified N_R (and in the Rhodes and Cyprus cases also FWI), we simulated different groundwater management scenarios for each site, in terms of different combinations of the managed pumping and artificial recharge rates, Q_P and Q_R, as summarized in Table 2. The site-specific locations of simulated pumping and recharge wells ($R(X_R,Z_R)$ and $P(X_P,Z_P)$ in Figures 1 and 2) remained the same for all simulated management scenarios listed in Table 2 and were determined within the WASSER project from known, site-specific well location and pumping rate distributions, and from groundwater dynamics investigations of associated efficient recharge well locations (Koussis 2001; Prieto 2001; Koussis et al. 2002).

In all three case studies, groundwater pumping and possible artificial recharge over the considered aquifer simulation domains do presently take place in wells that are quite evenly distributed along the coastline and around the simulated representative well locations. For such relatively uniform well rate and location distributions, the use of a representative two-dimensional groundwater simulation domain appears justified for the main interest of this paper, which is to quantify coastline and temporally integrated and averaged SGD values, representative of an entire coastal system. It appears generally unlikely that total groundwater pumping and artificial recharge, in amounts that are significant by relative to the total natural groundwater recharge and boundary inflow in a coastal aquifer, would take place in only one, or a few individual wells. Should this anyhow be the case, or if one's interest is to quantify local SGD fluxes, a detailed three-dimensional groundwater simulation model would be required for quantifying singular well influence zones and corresponding details of SGD variability along the coastline.

Results

The combined analysis of simulation results from all considered management scenarios in all three case studies showed an overall SGD pattern emerging in terms of the independent master variable:

$$Q_N \equiv \text{FWI} + N_R + Q_R - Q_P = \text{SGD} - \text{SWI} \tag{4}$$

which will in the following be referred to as the net land-determined groundwater drainage. The Q_N value is independent because all of its component flow rates can be estimated independently, by off-line catchment-scale hydrologic modeling and known groundwater management practices, as discussed above. The second equality in Equation (4) follows from a corresponding re-arrangement of the water balance Equation (1) and shows that the land-determined groundwater drainage Q_N must, at steady-state, equal the net seawater outflow rate, SGD − SWI.

Figure 3 shows the SGD simulation results for all considered groundwater management scenarios in all three sites (Table 2) as function of Q_N, at the resulting steady-state after subjecting a variety of steady-state (filled symbols in Figure 3) or arbitrary (open symbols in Figure 3) initial conditions to a step change in Q_N.

Figure 3(a) shows the results for site-realistic management practices (i.e., no more artificial recharge than locally available pumped groundwater, $Q_R \leq Q_P$ in Table 2), which for all investigated case studies yield relatively small Q_N values ($-400\,m^3\,year^{-1}\,m^{-1} < Q_N < 800\,m^3\,year^{-1}\,m^{-1}$, Table 2) and the best linear fit (solid line in Figure 3(a)):

$$\begin{aligned} SGD &= 1.3 \cdot Q_N + 390\,m^3\,year^{-1}\,m^{-1}; R^2 = 0.98; \\ &-400\,m^3\,year^{-1}\,m^{-1} < Q_N < 800\,m^3\,year^{-1}\,m^{-1} \end{aligned} \tag{5a}$$

Figure 3(b) shows all simulation results, including extended simulations for site-unrealistic water management practices ($Q_R > Q_P$ in Table 2) that yield large Q_N values ($Q_N > 800\,m^3\,year^{-1}\,m^{-1}$, Table 2), and the best linear fitting to all results (solid line in Figure 3(b)):

$$\begin{aligned} SGD &= 1.1 \cdot Q_N + 470\,m^3\,year^{-1}\,m^{-1}; R^2 = 0.998; \\ &-400\,m^3\,year^{-1}\,m^{-1} < Q_N < 10,000\,m^3\,year^{-1}\,m^{-1} \end{aligned} \tag{5b}$$

For comparison, fitting over the entire Q_N range to each individual site case yields site-specific regression lines (not shown in Figure 3) that are very similar to Equation (5b): $SGD = 1.1 \cdot Q_N + 516\,m^3 year^{-1}\,m^{-1}$ with $R^2 = 0.999$ for Israel; $SGD = 1.1 \cdot Q_N + 446\,m^3 year^{-1} m^{-1}$ with $R^2 = 0.999$ for Rhodes; and $SGD = 1.1 \cdot Q_N + 480\,m^3\,year^{-1} m^{-1}$ with $R^2 = 0.998$ for Cyprus.

The results summarized in Figure 3 and linear regression Equations (5) thus indicate that SGD is essentially linear in the net land-determined drainage, Q_N, with two characteristic slopes that are quite independent of site-specific details of hydrogeology and management scenario, or of the specific reason for the Q_N change from any initial to some new conditions. The two characteristic slopes depend only on Q_N value, with the slightly higher slope around the origin indicating some non-linearity in SGD for small Q_N. Both characteristic lines shown in Figure 3 (as well as all site-specific regression lines) imply that even if Q_N is decreased to zero by extracting a groundwater amount that corresponds to the total available fresh groundwater flow, the resulting SGD will still be greater than zero, and about $400\,m^3\,year^{-1}\,m^{-1}$ coastline width (from Figure 3(a), which is more accurate for small Q_N values). Furthermore, Figure 4 shows that the resulting freshwater fraction, SGD_F/SGD, of this total SGD may be up to 30%. The resulting overall behavior of SGD_F/SGD according to Equation (3) appears, in analogy with the total SGD results, to also be quite independent of field case, exact scenario details and initial conditions (Figure 4).

If $Q_N = 0$ while SWI $\neq 0$, it follows from Equation (4) that the SGD rate must then also be non-zero, that is, $SGD = SWI \neq 0$. Figure 5 illustrates the resulting steady-state streamlines (Figure 5(a)) and salt concentration isolines (Figure 5(b)) for the example $Q_N = 0$ simulation scenario of the Cyprus case study (Table 2). The streamlines in Figure 5(a) show that SWI $\neq 0$ and supplies a seawater fraction to the total pumped groundwater, Q_P, while some fresh water streamlines evade pumping, due to the natural and artificial recharge downstream of the pumping

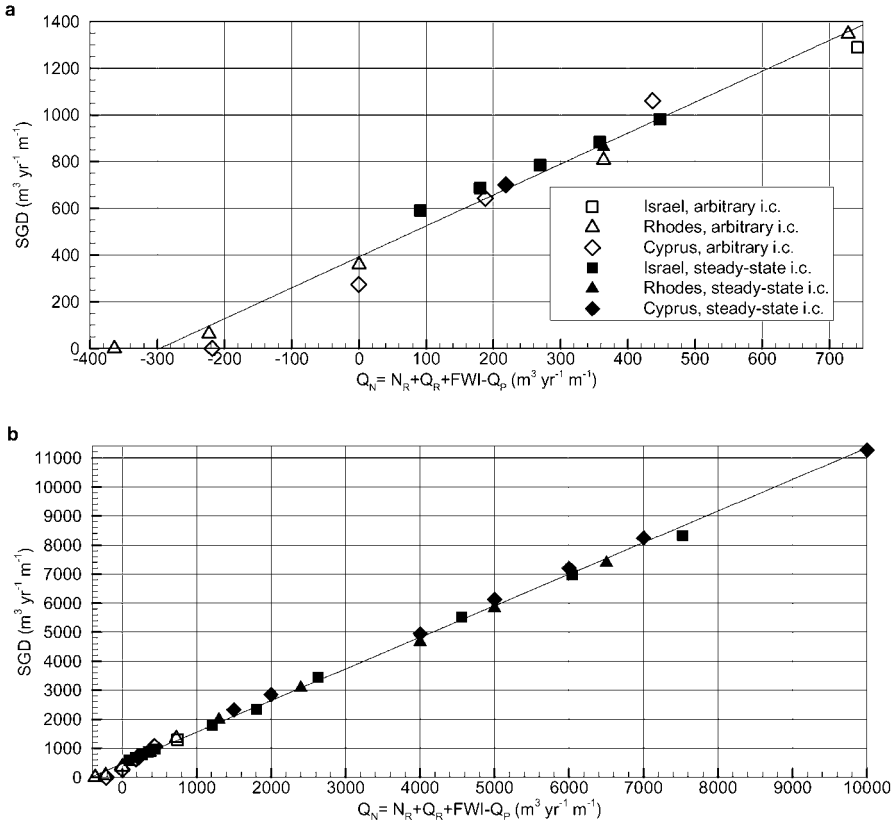

Figure 3. Resulting relation between SGD and prevailing Q_N at steady-state in all three case studies, with symbols: squares for Israel, triangles for Rhodes, and diamonds for Cyprus, and with filled symbols indicating simulations starting from steady-state initial conditions and open symbols indicating simulations starting from arbitrary initial conditions in all three cases; the Q_P, Q_R, N_R and FWI definitions are as in Figure 1. Part (a) shows results for site-realistic management practices ($Q_R \leq Q_P$, and resulting $-400\,m^3\,year^{-1}\,m^{-1} < Q_N < 800\,m^3\,year^{-1}\,m^{-1}$, Table 2), with linear fit (solid line) $SGD = 1.3 \cdot Q_N + 390\,m^3\,year^{-1}\,m^{-1}$, $R^2 = 0.98$; and part (b) shows all the results, including those for site-unrealistic water management practices ($Q_R > Q_P$, $Q_N > 800\,m^3\,year^{-1}\,m^{-1}$, Table 2), with linear fit $SGD = 1.1 \cdot Q_N + 470\,m^3\,year^{-1}\,m^{-1}$, $R^2 = 0.998$.

location, and flow into the sea instead. This evading freshwater yields the almost 30% freshwater fraction shown in Figure 4 for $SGD \approx 400\,m^3\,year^{-1}\,m^{-1}$, which corresponds to $Q_N = 0$ (Figure 3(a)).

For large Q_N values, we see by comparison of the second equality in Equation (4) (yielding SWI = SGD - Q_N) to the linear Equation (5(b)) that $SWI \approx 0.1 \cdot Q_N + 500\,m^3\,year^{-1}\,m^{-1}$. Figure 6(a) shows the resulting steady-state streamlines for the example $Q_N = 5000\,m^3\,year^{-1}\,m^{-1}$ simulation scenario of the Cyprus case study (Table 2), implying $SWI \approx 0.1 \cdot Q_N + 500\,m^3 \cdot\ year^{-1}\,m^{-1} = 1000\,m^3\,year^{-1}\,m^{-1}$,

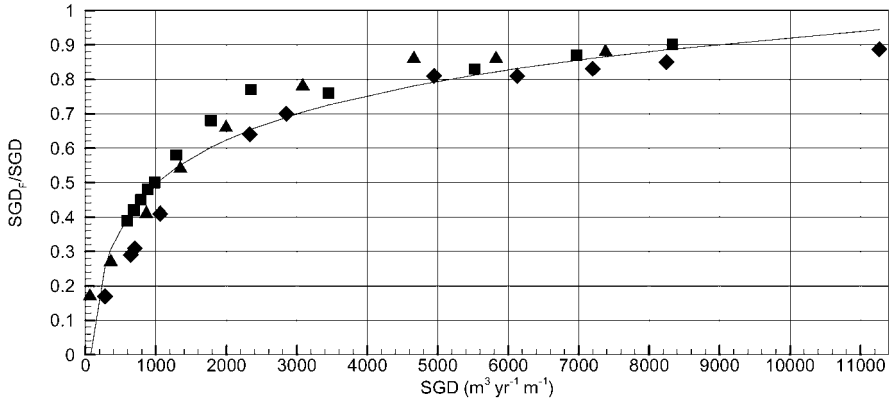

Figure 4. Resulting relation between the freshwater fraction SGD_F/SGD and total SGD in all three case studies, with symbols: squares for Israel, triangles for Rhodes, and diamonds for Cyprus. For illustrative purposes we also compare these results with the logarithmic curve $SGD_F/SGD = 0.185\ln(SGD) - 0.78$ (solid line, $R^2 = 0.92$).

total SGD $\approx 6000\,m^3\,year^{-1}\,m^{-1}$ (Eq. 5(b)), and resulting freshwater fraction $SGD_F/SGD \approx 5000/6000 = 0.83$; this freshwater fraction value is consistent with the general salt balance results from Equation (3) shown in Figure 4. The streamlines in Figure 6(a) then show that the seawater component of $1000\,m^3\,year^{-1}\,m^{-1}$ discharges into the sea in a seepage zone that extends much further seaward than the seepage zone for the SGD freshwater component of remaining $5000\,m^3\,year^{-1}\,m^{-1}$. Both the streamlines and the associated salt concentration isolines in Figure 6(b) also show that this seawater has essentially not been mixed with any freshwater, or flown through any aquifer sediments on the landside and can therefore not be used for explaining reported observations of excess coastal transport of tracer that has been desorbed from the aquifer by brackish-salt groundwater (Moore 1996).

For direct flow rate comparison, the total SGD rate of $3{\cdot}10^7\,m^3\,day^{-1}$, required for explaining the observed ^{226}Ra excess in coastal water (Moore 1996), corresponds to a coastline-averaged (over the 320 km coastline) SGD rate of $34{,}220\,m^3\,year^{-1}\,m^{-1}$. This SGD rate is almost 6 times greater than the SGD rate yielding the streamline and concentration isoline situation that is illustrated in Figure 6. Such a high SGD rate would according to the results shown in Figure 4 consist almost entirely of fresh groundwater ($Q_N \approx 30{,}000\,m^3\,year^{-1}{\cdot}m^{-1}$ according to Eq. 5(b)) with some additional (about $4000\,m^3\,year^{-1}\,m^{-1}$) seawater being measurable as SGD further seaward, however without having intruded into the aquifer (in analogy with Figure 6).

Relaxing the simplifying assumption of essentially homogeneous aquifers, which has been made in the present simulations, is not expected to considerably change the above results. Stochastic simulations have been made of the same three aquifer sites and simulation domains (Figure 2), under different water management conditions than those listed in Table 2 and considering both random spatial aquifer heterogeneity and random temporal hydrologic variability (Koussis 2001; Prieto 2001; Prieto C.,

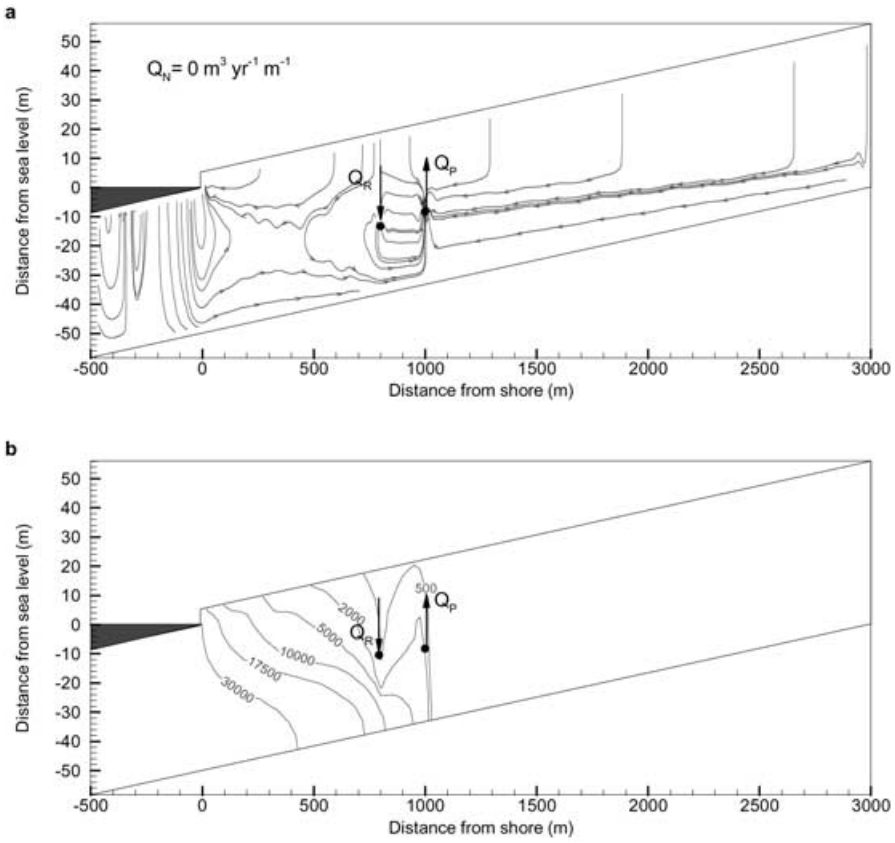

Figure 5. Steady-state results for the simulation scenario $Q_N = 0$ in the Cyprus case study (Q_N is defined as in Figure 3; see also scenario definition in Table 2, the resulting SGD value for the Cyprus case symbol at $Q_N = 0$ in Figure 3 and the corresponding freshwater fraction SGD_F/SGD in Figure 4), in terms of resulting steady-state: (a) streamlines, and (b) salt concentration isolines.

Destouni G., and Kotronarou A., Effects of coupled spatial–temporal randomness on seawater intrusion in three coastal aquifer cases, in review for publication 2003). These stochastic simulations yielded coefficients of variation in the point values of salt concentrations (i.e., concentrations in pumped groundwater) that were generally smaller than 100% (i.e., less than a factor two standard deviation from the mean salt concentration) for all three site cases and heterogeneity assumptions. The uncertainty in large-scale flow and transport quantities, such as the coastline-integrated and averaged SGD considered here, should generally be much smaller than for the point values of salt concentration, that is, much smaller than the factor 2 found for the latter. For solute transport in randomly heterogeneous soils and aquifers, it has been shown that uncertainty in large-scale discharge values, as quantified by the coefficient of variation from stochastic simulations, becomes negligible for spatial integration over

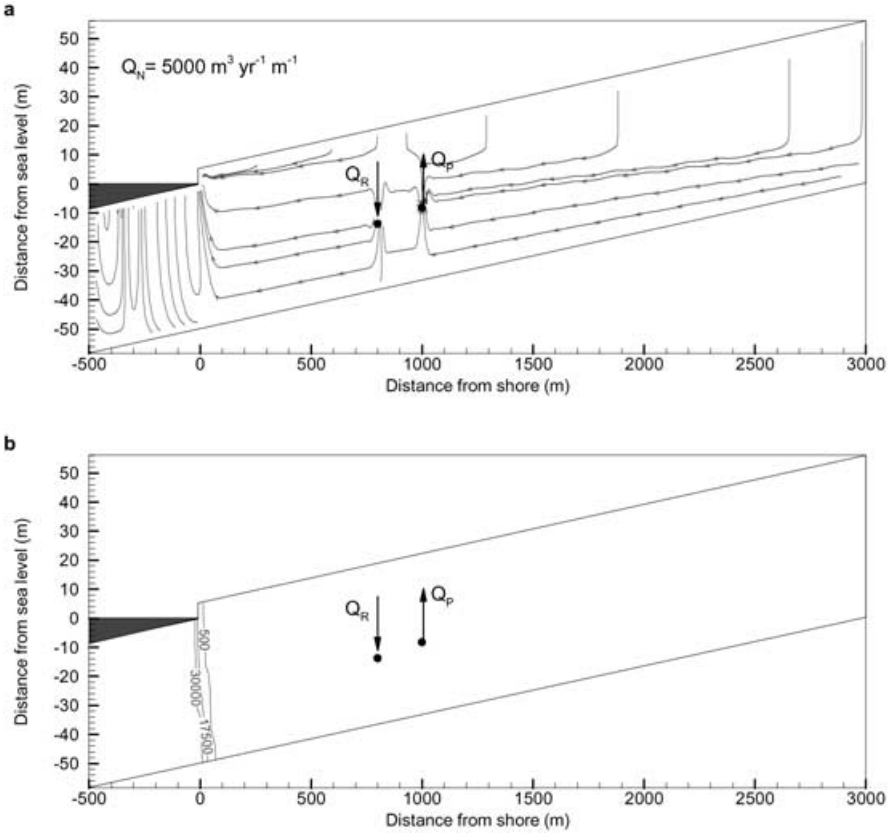

Figure 6. Steady-state results for the simulation scenario $Q_N = 5000\,m^3\,year^{-1}\,m^{-1}$ in the Cyprus case study (Q_N is defined as in Figure 3; see also scenario definition in Table 2, the resulting SGD value for the Cyprus case symbol at $Q_N = 5000\,m^3\,year^{-1}\,m^{-1}$ in Figure 3 and the corresponding freshwater fraction SGD_F/SGD in Figure 4), in terms of resulting steady-state: (a) streamlines, and (b) salt concentration isolines.

twenty, or more correlation lengths of hydraulic conductivity (e.g., Cvetkovic et al. 1992; Destouni 1992); noting that the hydraulic conductivity correlation length is typically in the range 1–10 m, we see that estimates of large-scale SGD value, integrated and averaged over a several kilometers long coastline, should not imply any great uncertainty due to aquifer heterogeneity.

Conclusions

We show that, once a steady-state SGD prevails, or is approached after some water management or hydrologic change, this SGD value can be modeled and predicted

by simple linearity in the net land-determined groundwater drainage Q_N, defined as the total fresh water drainage minus groundwater extraction. This linear relation appears to be independent of site-specific aquifer hydraulic characteristics, water management practices, or reason for a possible Q_N change from one steady-state to another.

Furthermore, the results imply that even if Q_N is decreased to zero, by extracting a groundwater amount equal to the total available fresh groundwater flow, the resulting SGD will still be greater than zero (about $400\,m^3\,year^{-1}\,m^{-1}$ coastline width), containing mostly seawater, but also a significant non-zero fresh water fraction (about 30%). If Q_N and thereby SGD are instead large, the fresh water fraction will also be large and quite insensitive to Q_N changes, but total SGD will still include some seawater (around 10% for our simulation limits), which would be measurable over a much greater seaward extent than the seepage zone for the fresh SGD component.

Independently of site-specific details, low average SGD and thereby low average Q_N will generally imply high average seawater content, because the fresh groundwater discharge will be too small to prevent the heavier seawater from intruding into the aquifer and mixing with the fresh water within a wide salinity transition zone of brackish groundwater. Increasing SGD implies decreasing seawater content, increasing efficiency in preventing seawater intrusion and mixing with fresh water, and narrowing of the salinity transition zone between seawater and fresh groundwater.

Thereby, very large average SGD values are inconsistent with the high seawater content and the wide salinity transition zone that are also required for explaining reported observations of excess desorbed tracer transport from coastal aquifers into the coastal water (Moore 1996). Tidal oscillation and other possible causes for temporal SGD variability around its annual average value may provide at least a partial explanation for such observations, by temporarily allowing for large SGD with large seawater component to occur, due to the return flow of seawater that intruded into the aquifer during previous periods of low SGD. This possible explanation needs further investigation and the modeling approach presented here provides a good basis for extending the present steady-state analysis into temporal variability effects.

In addition, there is also a need to further investigate the possibility that excess tracer transport from aquifers into coastal waters may be the result of ongoing seawater intrusion due to small (rather than to extremely large) direct SGD. Specifically, low SGD implies formation of a wide salinity transition zone in the aquifer, from which desorbed tracer may be transported into the sea by indirect groundwater flow, through groundwater inflow into stream stretches within this transition zone and then into the coastal water. Such an explanation would be consistent with resent observations and model interpretation of stream chemistry, showing that solute transport by groundwater flow into streams and rivers may be far more important for feeding surface water flow and solute transport, even during high flow periods, than traditionally believed and modeled (Kirchner et al. 2000, 2001).

Acknowledgements

We thank the Swedish Research Council (VR) for their financial support of the present SGD investigations. We thank SCOR and LOICZ for sponsoring the Working Group 112, Magnitude of Submarine Groundwater Discharge and its Influence on Coastal Oceanographic Processes and facilitating fruitful and helpful discussions, problem definitions and collaborations within the group; SCOR is funded in part by the National Science Foundation under Grant No. 0003700. We also gratefully acknowledge the contribution of the WASSER consortium to the conceptualization and data support of the three case studies, and the financial support of WASSER by the European Commission's Directorate General for Research (DG12), under contract ENV4-CT97-0459.

References

Buddemeier R.W. 1996. Groundwater flux to the Ocean: definitions, data, applications, uncertainties. In: Buddemeier R.W. (ed) Groundwater Discharge in Coastal Zone: Proceedings of an International Symposium. LOICZ Reports and Studies No. 8, LOICZ, Texel, The Netherlands, pp. 16–21.

Cvetkovic V., Shapiro A. and Dagan G. 1992. A solute flux approach to transport in heterogeneous formations, 2, Uncertainty analysis. Water Resour. Res. 28: 1377–1388.

Destouni G. 1992. Prediction uncertainty in solute flux through heterogeneous soil. Water Resour. Res. 28: 793–801.

Kirchner J.W., Feng X. and Neal C. 2000. Fractal stream chemistry and its implications for contaminant transport in catchments. Nature 403: 524–527.

Kirchner J.W., Feng X. and Neal C. 2001. Catchment-scale advection and dispersion as a mechanism for fractal scaling in stream tracer concentrations. J. Hydrol. 254: 82–101.

Koussis A.D. (ed) 2001. WASSER: Utilisation of groundwater desalination and wastewater reuse in the water supply of seasonally-stressed regions. Final report to the European Commission DG XII-D, Environment and Climate Programme, Contract No. ENV4-CT97-0459. National Observatory of Athens.

Koussis A.D., Kotronarou A., Destouni G. and Prieto C. 2002. Intensive groundwater development in coastal zones and small islands. In: Llamas R. and Custodio E. (eds) Groundwater Intensive Use: Challenges and Opportunities. Balkema ISBN: 90 5809 390 5, The Netherlands, pp. 133–155.

Leavesley G.H. and Stannard L.G. 1995. The precipitation–runoff modeling system – PRMS. In: Singh V.P. (ed) Computer Models of Watershed Hydrology. Water Resources Publications. Forth Collins, Colorado, pp. 281–310.

Leavesley G.H., Lichty R.W., Troutman B.M. and Saindon L.G. 1983. Precipitation-runoff modeling system. User's manual. U.S. Geological Survey Water Resources Investigations 83-4238, 207 p.

Leavesley G.H., Markstrom S.L., Brewer M.S. and Viger R.J. 1996a. The modular modeling system (MMS) – The physical process modeling component of a database centered decision support system for water and power management. Water Air Soil Pollut. 90 (1–2): 303–311.

Leavesley G.H., Restrepo P.J., Markstrom S.L., Dixon M. and Stannard L.G. 1996b. The modular modeling system – MMS. User's manual. U.S. Geological Survey Open File Report 96-151, 142 p.

Leavesley G.H., Markstrom S.L., Restrepo P.J. and Viger R.J. 2002. A modular approach to addressing model design, scale, and parameter estimation issues in distributed hydrological modelling. Hydrol. Processes 16(2): 173–187.

Li L., Barry B.A., Stagnitti F. and Parlange J.-Y. 1999. Submarine groundwater discharge and associated chemical input to a coastal sea. Water Resour. Res. 35: 3253–3259.

Moore W.S. and Church T.M. 1996. Submarine groundwater discharge. Reply to Younger (1996). Nature 382(6587): 122.

Moore W.S. 1996. Large groundwater inputs to coastal waters revealed by Ra enrichments. Nature 380: 612–615.

Moore W.S. 1999. The subterranean estuary: a reaction zone of ground water and sea water. Mar. Chem. 65(1–2): 111–125.

Neitsch S.L., Arnold J.G. and Williams J.R. 1999. Soil and water assessment tool. User's manual, v. 98.1. Agricultural Research Service and Texas Agricultural Experiment Station, Temple, Texas.

Prieto C. 2001. Modelling freshwater–seawater interactions in coastal aquifers: long-term trends and temporal variability effects. Licentiate Thesis. Department of Civil and Environmental Engineering, Royal Institute of Technology, Stockholm, Sweden.

Prieto C., Destouni G. and Schwarz J. 2001. Seawater intrusion in coastal aquifers: effects of seasonal variations in extraction and recharge rates. In: Ouazar D. and Cheng A.H.-D. (eds) SWICA M^3 Cyber Proceedings of First International Conference on Saltwater Intrusion and Coastal Aquifers – Monitoring, Modeling, and Management, Essaouira, Morocco, 23–25 April, 2001. Available online at http://www.olemiss.edu/sciencenet/saltnet/page8.html.

Simmons G.M. 1992. Importance of submarine groundwater discharge (SGWD) and seawater cycling to material flux across sediment/water interfaces in marine environments. Mar. Ecol. Prog. Ser. 84: 173–184.

Tahal Consulting Engineers Ltd. 1999. Israel case study. Complementary data-I. 1st WASSER progress report, Annex VII, Volume IV.

Uchiyama Y., Nadaoka K., Rölke P., Adachi K. and Yagi H. 2000. Submarine groundwater discharge into the sea and associated nutrient transport in a sandy beach. Water Resour. Res. 36: 1467–1479.

Voss C.I. 1984. Saturated–Unsaturated TRAnsport. U.S. Geological Survey Water-Resources Investigations Report 84-4369, USGS.

Younger P.L. 1996. Submarine groundwater discharge. Nature 382(6587): 121–122.